



**Label-Free High-Throughput Detection and Content Sensing
of Individual Droplets in Microfluidic Systems**

Journal:	<i>Lab on a Chip</i>
Manuscript ID:	LC-ART-03-2015-000314.R3
Article Type:	Paper
Date Submitted by the Author:	04-Aug-2015
Complete List of Authors:	Yesiloz, Gurkan; University of Waterloo, Mechanical and Mechatronics Engineering Boybay, Muhammed; Antalya International University, Computer Engineering Ren, Carolyn; University of Waterloo,

ARTICLE

Label-Free High-Throughput Detection and Content Sensing of Individual Droplets in Microfluidic Systems

Cite this: DOI: 10.1039/x0xx00000x

Gurkan Yesiloz,^a Muhammed Said Boybay^{a,b} and Carolyn L. Ren^{*a}Received 20th February 2015,
Accepted 00th January 2015

DOI: 10.1039/x0xx00000x

www.rsc.org/

This study reports a microwave-microfluidics integrated approach capable of performing droplet detection at high-throughput as well as content sensing of individual droplets without chemical or physical intrusion. The sensing system consists of a custom microwave circuitry and a spiral-shaped microwave resonator that is integrated with microfluidic chips where droplets are generated. The microwave circuitry is very cost effective by using off-the-shelf components only. It eliminates the need for bulky benchtop equipment, and provides a compact, rapid and sensitive tool compatible for Lab-on-a-Chip (LOC) platforms. To evaluate the resonator's sensing capability, it was first applied to differentiate between single-phase fluids which are aqueous solutions with different concentrations of glucose and potassium chloride respectively by measuring its reflection coefficient as a function of frequency. The minimum concentration assessed was 0.001 g/ml for potassium chloride and 0.01 g/ml for glucose. In the droplet detection experiments, it is demonstrated that the microwave sensor is able to detect droplets generated at as high throughput as 3.33 kHz. Around two million droplets were counted over a period of ten minutes without any missing. For droplet sensing experiments, pairs of droplets that were encapsulated with biological materials were generated alternatively in a double T-junction configuration and clearly identified by the microwave sensor. The sensed biological materials include fetal bovine serum, penicillin antibiotic mixture, milk (2%mf) and D-(+)-Glucose. This system has significant advantages over optical detection methods in terms of its cost, size and compatibility with LOC settings and also presents significant improvements over other electrical-based detection techniques in terms of its sensitivity and throughput.

Introduction

In recent years, there has been growing interest in droplet-based microfluidics because of its promise to facilitate a broad range of scientific research and biological/chemical processes. Potential applications can be found in many areas such as cell analysis^{1,4}, DNA hybridization⁵, detection of bioassays⁶, bio-reactions⁷⁻⁹, drug screening¹⁰ and diagnostics^{11,12}. Major advantages of droplet-based microfluidics versus traditional bioassays include its capability to provide highly uniformed, well isolated environment for reactions with orders of magnitude higher throughput (i.e. kHz). Most droplet-based microfluidic studies rely on high speed imaging¹³⁻¹⁷ to provide details of droplet generation and transport, which usually require expensive and bulky high speed camera, and exhaustive post imaging analysis. In addition, in order to differentiate subtle differences in droplet content, fluorescent imaging is often used which, however, tends to lower down the throughput because longer residence time is needed for the droplet to stay in the field of view in order to obtain sufficiently high fluorescent intensity. Although this can be improved by using a

pulse solid state laser that is synchronized with the camera, which further complicates the system due to the need for precise alignment and fluorescent labelling.

In contrast, electrical techniques allow the miniaturization of multiple sensor arrays and their integration into one single microfluidic chip with low power requirement. Of these capacitive, electrochemical and impedance based electrical detection methods are widely available. In electrochemical detection, the measurements are based on the interactions between analytes and electrodes or probes that usually occur in an electrolytic cell. They are not able to distinguish analytes that are not electroactive¹⁸⁻²⁰. In addition, the detection electrodes are sensitive to variations in temperature, ionic concentration and pH that affect the shelf life of the sensor and shift electrodes' response requiring frequent calibration^{18, 21-22}. Conventional capacitive and impedance detection approaches operate at low frequencies, which causes either low signal-to-noise ratio or long response time and thus limit their applications to droplet microfluidics where droplets are generated at high frequencies. For example, the throughput achieved by a capacitive sensor²³ for droplet detection was up

to 90 Hz with reasonable sensitivity and for an electrical impedance-based detection²⁴ around 10.

Microwave technology, as a versatile non-optical method, has the potential to address the above issues because it eliminates the need for chemical modification or physical intrusion of the sample and operates at high frequencies (i.e. GHz). It differentiates materials based on their electrical properties including electrical conductivity and/or dielectric constant. Previously we demonstrated a microwave sensor that can be integrated with microfluidic devices to differentiate single phase fluids in microchannels and detect the presence of droplets at a very low frequency (i.e. up to 1.25 Hz)²⁵. The low detection frequency was mainly restricted by the response time of the vector network analyzer (VNA). In addition, the sensing of droplet content was not achieved because insufficient sampling of droplets did not allow the accurate determination of the time for the droplet to arrive at the capacitive gap, neither differentiation of the content changes²⁵. Also, in order to get a reliable reading by the microwave sensor, the effect of droplet geometry on sensing performance must be eliminated, and the sensitivity of the microwave sensor must be sufficiently high to detect subtle variations.

In this study, we present a sensitive, low-cost, portable microwave circuitry suitable for detection of droplet presence and label-free sensing of individual droplet content in microfluidic devices. More importantly, for future point-of-care application purposes, we limited ourselves to the choices of cost-effective off-the-shelf components for developing the circuitry. Basically the circuitry that consists of surface mount components is able to generate microwave signal and measure the response of the sensor (reflection coefficient of the sensor) in a very fast manner. We validated that the system has a detection limit of several kilohertz (kHz) itself, and in the experiments we reached over 3 kHz. This microfluidic-microwave system might potentially be used as a coulter counter and content analysis in many applications.

Description of Methods and Materials

System Overview

The system illustrated in Fig. 1 (please see supplemental material Fig.S1 for the image of the entire setup) consists of a microfluidic chip integrated with a microwave sensor, a pumping unit which could be a pressure controller (Fluigent MFCS-8C) or a syringe pump (Pump33, Harvard Apparatus) depending on the particular study case, an inverted microscope (Eclipse Ti, Nikon) mounted with a high-speed camera (Phantom v210, Vision Research) and the developed microwave custom circuitry. Fluid reservoirs are connected to the microfluidic chip via ethyltrifluoroethylene (ETFE) tubing and connectors (Tefzel, Upchurch Scientific). Two slightly modified configurations (simple flow focusing and double T-junction) were used for droplet generation. For the detection of droplet presence, the simple flow focusing geometry was used while for the sensing of droplet content, the double T-junction geometry was used where droplets with different contents were alternatively generated by the two T-junctions. Droplet generation and transport were manipulated through the microfluidic channel network design by adjusting the pressures of the inlets or the pumping flow rate of the syringe pump. The high speed camera was used to record microscopic images and

videos through the image processing program ImageJ (National Institute of Health, MD, USA) which were also used to validate the experimental results obtained through the developed circuitry. A data acquisition device and Labview software (National Instruments) were used to control the system and set off the computer interface.

Materials

Fluorinated oil (FC40 from Sigma-Aldrich) with a 2% custom-made surfactant was used as the continuous phase. The surfactant has a chemical structure of PFPE-PEG-PFPE (or Krytox-Jeffamine-Krytox, where Krytox has a molecular weight of 7500 and Jeffamine 900). D-(+)-Glucose (Sigma-Aldrich) and potassium chloride (EMD Millipore) solutions were prepared in ultra-pure water. Penicillin-Streptomycin-Neomycin antibiotic mixture (containing 5,000 units penicillin, 5 mg streptomycin and 10 mg neomycin/mL), Fetal Bovine Serum (FBS; Sigma-Aldrich) and milk (contains 2%MF) were used in the sensing of droplet content without further purification or dilution.

For further demonstration of the developed system for potential bioapplications, Alzheimer's disease (AD) testing was chosen. Tau-derived hexapeptide (AcPHF6) which is used to model the tau-protein aggregation related to AD was purchased from Celtek Peptides. The assay was carried out with orange G, which is a known inhibitor to the tau-protein aggregation (Sigma-Aldrich). AcPHF6 was prepared in ultrapure water at a concentration of 2.5mg/ml as stock solution, and diluted to a final concentration of 0.316 mM. All other solutions were prepared in morpholinepropanesulfonic acid (MOPS) buffer with 0.01% Na₃N and adjusted to pH 7.2, and with assay grade DMSO at 1% (v/v).

Microwave Sensor

The designed microwave sensor works essentially as a resonator. The sensor structure is made of two concentric copper loops similar to the one presented previously²⁵. Microwave signal is excited by the outer coplanar transmission line loop, which supplies a time-varying oscillating current circulating around the loop and a magnetic field passing through the loop. The inner loop with a small gap constructs the resonator and the microchannel where droplets are passing through is aligned on top of this gap. When materials with different electrical properties (permittivity, conductivity) pass by the gap region, the capacitance of the gap changes and the resonance frequency shifts which can be used to characterize the materials. Take water-in-oil emulsion as an example, water droplets have a much higher dielectric constant (~80) than the carrier fluid, oil (~2-3). When a water droplet passes by the resonator, the resonance frequency will be shifted which can be used to detect droplet's presence. Similarly, when droplets with different materials pass by the resonator, the magnitude of shift in the resonance frequency can be used to characterize the droplet content. The resonance frequency shift caused by a perturbation in the permittivity of the medium is described by²⁶.

$$\frac{\Delta f}{f} = \frac{-\int_{V_0} \Delta \epsilon \vec{E} \cdot \vec{E}_0 dV}{\int_{V_0} (\epsilon \vec{E} \cdot \vec{E}_0 + \mu \vec{H} \cdot \vec{H}_0) dV} \quad (1)$$

where E_0 and E are the electric fields before and after the perturbation, H_0 and H are the magnetic fields before and after

the perturbation, f is the resonance frequency before the perturbation, ϵ is the permittivity of the medium and μ is the permeability of the medium. In this study, a spiral-shaped capacitive region was designed for sensing purposes because it allows the system to operate at lower frequencies compared to T-shaped designs²⁵, which thus allows inexpensive off-the-shelf components to be chosen for the circuitry design.

Fabrication

The microfluidic chip consists of two main components, a glass base with the microwave components and a polydimethylsiloxane (PDMS) mold with the designed microchannels for droplet generation and transport, which are fabricated separately and then bonded together. Thus, the device fabrication consists of two stages: microchannel and microwave component fabrication.

0.1 M H₃BO₃, and 0.1 M H₂SO₄) and electroplated at 2 mA for 4 min and then 7 mA for 20 min as illustrated in Fig. S2 (please see supplemental material). After electroplating, the photoresist is removed with acetone leaving an electroplated copper film approximately 5 μ m thick. Next, the base layer of pre-deposited copper is removed by etching with dilute ferric chloride (5%) (MG Chemicals). A passivation layer of a mixture of PDMS (Sylgard 184, Dow Corning) and toluene (1:1 (w/w) PDMS/toluene) is spin-coated at 4000 rpm for 60 s followed by 1 hr curing at 95 $^{\circ}$ C to protect the electrical traces. A subminiature version A (SMA) connector (Tab Contact, Johnson Components) is then soldered to the electrodes of the microwave components to provide an external connection to the microwave circuitry.

Microchannel. Microchannels are fabricated from PDMS using standard soft-lithography techniques. The PDMS is mixed in a 10:1

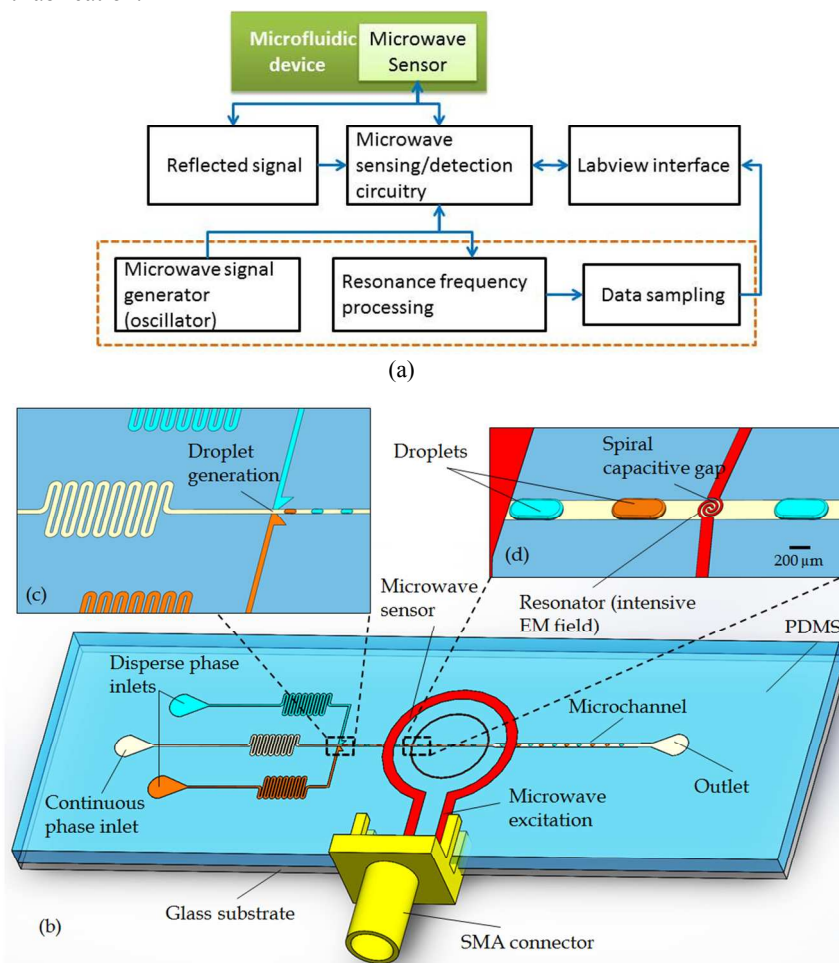


Figure 1. (a) A schematic of the microwave-microfluidics integrated device, (b) schematic of microwave sensor with a spiral resonator design and an excitation loop.

Microwave Component. The electrical traces for the microwave components are fabricated using a combination of photolithography and electroplating. Briefly, the positive photoresist, S1813 (Rohm-Haas), is spin-coated at 1500 rpm for 60 s onto a 50 nm thick copper film (EMF Corporation) that is pre-deposited on a glass slide and then baked at 95 $^{\circ}$ C for 120 s. The design is patterned into the photoresist via UV lithography and subsequently developed with MF-319 (Rohm-Haas) for 2 min. The patterned slide is then immersed in an acidic copper electroplating solution (0.2 M CuSO₄,

ratio of base to curing agent, degassed and molded against SU-8/silicon masters which are fabricated using the same procedure developed previously²³ and then cured at 95 $^{\circ}$ C for 2 h. The molds are then peeled off from the masters and fluidic access holes are made using a 1.5 mm biopsy punch. Both the finished microwave components and the PDMS mold are then treated with oxygen plasma at 29.7 W, 500 mTorr for 30 s. The plasma treatment process renders PDMS hydrophilic; however, for water in oil droplets, the PDMS channels should be hydrophobic to form droplets. For this

purpose, the walls of the microfluidic channels are coated with Aquapel (PPG Industries) to ensure that they are preferentially wet by the fluorinated oil.

Microwave Custom Circuitry

Vector Network Analyzers (VNAs) are widespread tools for microwave characterization due to their accuracy and user-friendly interface. However, VNAs are expensive normally which has driven the development of inexpensive alternatives²⁷⁻²⁹. Regular VNAs such as the one we used previously²⁵ have limitations on the data sampling rate and thus throughput which only allowed a very low throughput (i.e. up to 1.25 Hz for

the DAQ (0 - 10V) for tuning purposes. Tuning voltages are amplified by the op-amp with a gain factor of 2. The total amplified voltage ranging between 0 to 20V controls the tuning voltage of the VCO which is measured by the DAQ and LabView program and characterized by a spectrum analyzer (Agilent, E4440A). Serial capacitors are used in order to reduce the parasitic effects and filter the signal for the op-amp and VCO input. The microwave signal generator subsystem facilitates the sweeping over the desired frequency range (1.9 GHz to 2.6 GHz). We designed the sensor operating below 3 GHz at which the corresponding microwave components are widely available and inexpensive that allow the total cost of the electronic components below \$200. Wider frequency ranges can be achieved by adjusting the tuning voltage of the VCO.

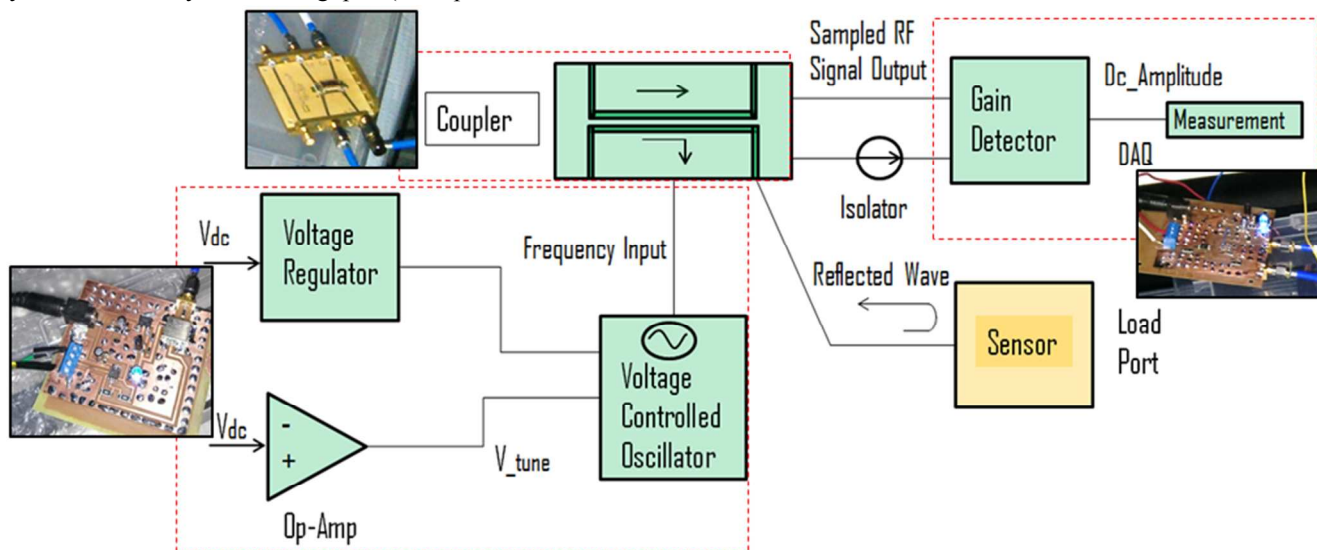


Figure 2. Schematic description of the microwave circuitry.

droplet detection). Another major disadvantage of such bulky benchtop setups is their size which makes it difficult to be widely applied for point-of-care applications. In this regard, it is necessary to develop portable yet affordable microwave circuitries that have comparable accuracy and sensitivity as commercially available VNAs. In this study, we report such a microwave circuitry for label-free detection and content sensing of droplets in microfluidic devices. Considering the microwave structure used in detecting and sensing droplets, a microwave circuit that measures the reflection coefficient from a one port network is designed since the change in the resonance frequency can be monitored in the reflection coefficient. The microwave circuitry is mainly composed of three sub-systems: i) signal generator, ii) power coupling unit, and iii) gain detector as shown in Fig.2.

i) Microwave Signal Generator

This subsystem consists of a voltage controlled oscillator (VCO) (Mini-Circuits, ROS-2350-519+), a voltage regulator (Rohm Semiconductor, BA17805FP-E2), a data acquisition system (DAQ) (National Instruments), an op-amp (Texas Instruments, LM358DR), and a power supply (24V battery) that supplies voltage to the op-amp and voltage regulator. The VCO provides the required microwave frequency by converting the input analog voltage, which consists of two components: one voltage source provided by the 24V power supply but regulated by the voltage regulator to the maximum of 5V and the other by

ii) Power Coupling

The primary function of the power coupling unit is to provide proper microwave signals to the sensor and the gain detector which would require careful isolation of signals without sacrificing the useful power. The high operating frequency at the GHz range brings in more challenges in the design and fabrication of the microwave components. First, the impedance of the transmission lines in the printed circuit board must match to the characteristic impedance of 50 Ω because any mismatch between the transmission line traces causes reflections and reduces the performance²⁷. For this purpose, 0.79 mm thick FR-4 PCB material ($\epsilon=4.34$) is used and microstrip impedances are carefully calculated considering the trace width, thickness and substrate height. The copper ground (at the bottom of the PCB) and ground planes (on the top of the PCB) are connected with vias closer to $1/20\text{th } \lambda$ where λ is the wavelength of the signal flowing through it to reduce noise³⁰. In order to minimize parasitic coupling to the transmission lines, separations between the ground planes and all other traces are designed to be at least three times larger than the substrate thickness. Second, reflections between different components must be controlled well which include the reflection from the attenuator, VCO, and directional coupler, to the microwave sensor which is connected to the circuitry through coaxial cables, and that from the microwave sensor back to the VCO which have disturbing effects on robust frequency generation. The above concerns are taken into consideration in the design of the power coupling

and isolator subsystem. Specifically, a high directivity bi-directional coupler (Mini-Circuits, SYBD-16-272HP+) with 16 dB coupling is used to regulate microwave power to the resonator. Additionally, a 20 dB resistive attenuator is used as an isolator network which is chosen to isolate the reflected signal because of the mismatch of the sensor while not reducing the useful power significantly.

iii) Gain Detector

An integrated circuit (Analog Devices, AD8302) is employed in the gain detection subsystem which communicates with the microwave sensor and the power coupling unit. The signal traveling from the signal generator is coupled by the bi-directional coupler to the gain detector as a reference signal and to the resonator which is aligned with microchannel. Then the gain detector enables the amplitude and phase difference between the signal reflected from the sensor and the reference signal to be measured which is described by the reflection coefficient.

$$\Gamma = \frac{\text{Reflected Voltage}}{\text{Incident Voltage}} = \frac{(Z_R - Z_0)}{(Z_R + Z_0)} \quad (2)$$

where Z_R is the frequency dependent input impedance of the device presented in Fig. 1(b) that includes the resonator and the excitation structure and Z_0 is the characteristic impedance of the transmission line used for feeding the structure. The gain detector converts the microwave signals to DC signal, and this magnitude ratio of electronic signal is post-processed and used to relate nanoliter-sized droplet detection and sensing of its content. For example, if different materials pass by the sensor,

the reflected signal would be different even though the incident voltage would be the same which can be used for detection and sensing of materials. The system is able to detect ac-coupled input signals from -60 dBm to 0 dBm. The output reflection coefficient range can be accurately measured between -30 dB to +30 dB which is scaled to 30mV/dB. The system is also able to measure the phase over a range of 0° – 180° . The minimum and maximum levels of the detection limits are characterized by the limit that each individual log amp can detect as well as the finite directivity of the coupler.

The LabVIEW program is used as an interface to collect and convert the measurement data, and control the system real time. Meanwhile, a calibration algorithm is used to correlate the measured data readings of the gain detector to the reflection coefficient of the microwave sensor which carry the information of the physical droplet system (Fig.S1).

Results and Discussion

Characterization of Microwave Circuitry

Prior to the droplet detection and sensing using the developed microwave circuitry, its sensitivity and accuracy was first evaluated by comparing its measurement results with that obtained using a commercial VNA (MS2028C, Anritsu). Table 1 below shows the comparison of the measured resonance frequencies for FC-40 ($\epsilon=1.9$), air ($\epsilon=1$), and water ($\epsilon=78.54$) between the custom-made circuitry and VNA. The developed microwave circuitry has very similar performance to the commercial VNA with the maximum difference of 1.283% found for water.

Then the detection and counting function of the developed

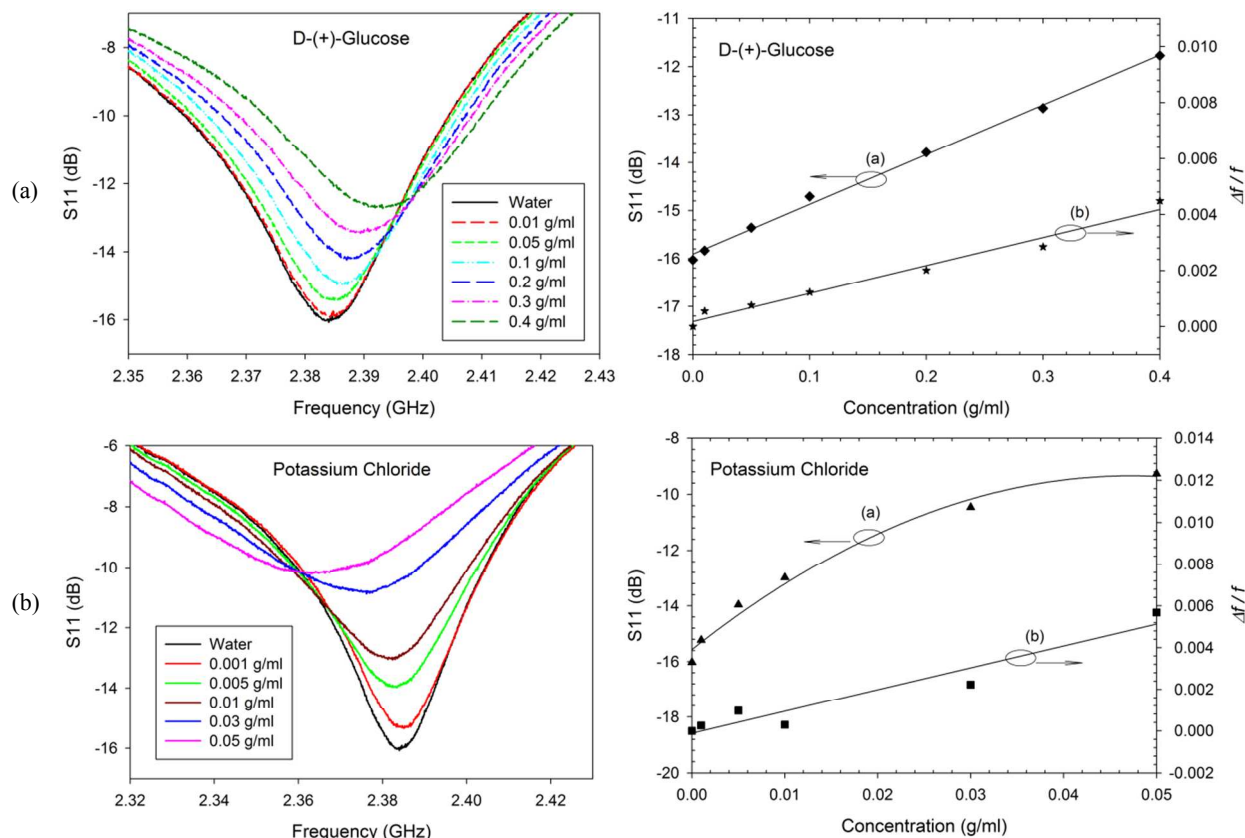


Figure 3. Reflection coefficient of the resonator for a series of Glucose-Water (a) and KCl-Water (b) mixtures for testing the circuitry.

circuitry was thoroughly evaluated by measuring the reflection coefficient of the resonator for various fluids in microchannels as a function of frequency. In order to prevent potential contamination caused by the residual of the previous sample; the microchannels were primed with the solution to be tested for at least 15 min prior to each test, and flushed with oil for 10 min. The tubing was cleaned twice before measurements by purging air and then with isopropanol.

Table 1. Comparison of the resonance frequencies between custom design and the VNA.

Material (Liquid)	f@S11 min using VNA (MHz)	f@S11 min using Custom Design (MHz)	Variation Percentage (%)
Air	2588	2580	0.309
FC-40	2582	2573	0.349
Water	2417	2386	1.283

solutions (KCl) were prepared with ultra-pure water. The minimum assessed concentration is 0.001 g/ml for KCl and 0.01 g/ml for glucose. The frequency step size was 0.1 MHz in the analysis. The lower detection limit was achieved for the KCl solutions because of the combined effects of permittivity and ionic conductivity (dominant effect). For example, the conductivity of potassium chloride increase from 17.84 mS/cm to 60.8 mS/cm when its concentration increases from 0.01g/ml to 0.05 g/ml, which were experimentally measured using a conductivity meter kit (Thermo Scientific, Orion 5-Star) after calibration of the probe with three different calibration solutions. While increasing KCl concentration causes a decrease in the resonance frequency, increase in the glucose concentration results in higher resonance frequencies (See S3 in the supplemental). As well, concentration changes cause sharp decline in the reflection coefficient (S_{11}) so that the change in resonance frequency can be monitored in the reflection coefficient. The differentiation of fluids with small differences in electrical properties validated the dynamic performance of the customized microwave circuitry along with the microwave sensor integrated with the microchannels.

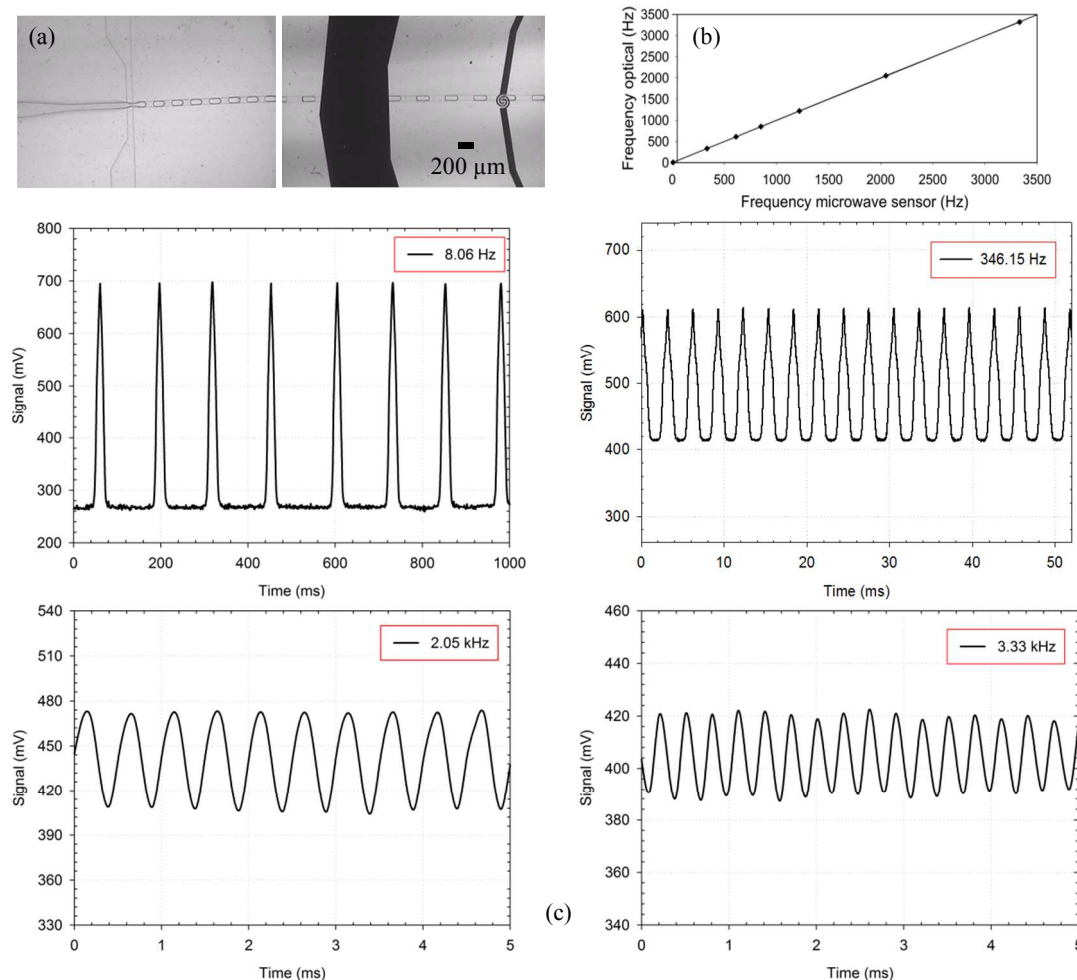


Figure 4. (a) Image of the generator and generated droplets, (b) comparison of the droplet generation frequencies; optical imaging vs. microwave sensor, (c) high-throughput droplet detection.

As shown in Fig.3, the circuitry is able to differentiate between fluids with permittivity effects dominant (Fig. 3a) and conductivity effects dominant (Fig. 3b). Different concentrations of D-(+)-Glucose and potassium chloride

High-Throughput Droplet Detection

The performance of the microwave circuitry for droplet detection and counting is performed using a flow focusing

generator as shown in Fig. 4. The channel height is 50 μm and assumed to be uniform across the entire chip. The channel width smoothly narrows down from 300 μm to 80 μm at the intersection which is the same as that of the dispersed phase for generating droplet stably. The wider channels were designed to lower down the hydrodynamic resistance for easy pumping while the uniform channel widths near the generator is the most stable design for droplet generation³¹. Initially, the droplet generation and transport were visualized and characterized with the optical microscope (Eclipse Ti, Nikon) integrated with a high speed camera which captured images at a frame rate of 9000 fps. Fig. 4 (a) shows the image of the generator and generated droplets which are around 1nl considering the droplets are fully confined by the channel (50 μm high, 80 μm wide) with a length varying from 1~3 channel widths (80 μm ~ 240 μm). Fig. 4 (b) compares the droplet generation frequencies measured by the optical imaging and microwave sensor.

When a droplet passes the capacitive region (gap) of the resonator, the electromagnetic field is disturbed by the presence of the droplet and the dielectric change (from the oil phase to the aqueous droplet phase) causes a peak in the collected signal. The perturbation in the EM field can be used to determine the droplet generation frequency by counting the number of the perturbations over a specific time period. As shown in Fig. 4 (c), the signal peaks correspond to droplet presence while the valleys correspond to the carrier fluid (oil). The resonator was operated at 2.59 GHz which was the resonance frequency for FC40 oil, and at this frequency the signal change in reflection coefficient is used to determine the droplet presence. It is worthy to mention that the sinusoidal look of peaks at very high droplet formation frequencies is caused by shorter and unstable droplet spacing which are likely due to the use of syringe pump which cause unpredictable uncertainties³¹. Due to the limitation of the maximum pressure that the pressure controller can provide which limits the throughput of droplet generation, a syringe pump was used in order to evaluate the detection performance of the microwave system. With carefully cleaning and preparation of microfluidic chips we reached as high flow rates as 4000 $\mu\text{l/hr}$ for water and 4750 $\mu\text{l/hr}$ for the continuous phase (i.e. oil). Correspondingly, we were able to generate droplets at the maximum rate of 3.33 kHz which can be detected with the microwave system successfully. Further high frequencies can be achieved by increasing the flow rate, which however tends to break chip made of PDMS³².

Ideally, in order to detect a droplet, at least one signal level needs to be sampled from carrier fluid and one from dispersed (droplet) phase. This will result to give a minimum and a maximum value, and maximum detection limit can be estimated to be the half of the signal generation rate provided that the data sampling rate of the system is equal or larger than signal generation rate. In our system, since the signal generation frequency is at microwave range (i.e., GHz), which is extremely higher than data sampling that the data sampling rate basically determines the maximum detectable limit. However, since the droplet spacing is low in our very high droplet generation frequencies because of the droplet generation limitations explained above, the collected data gives a sinusoidal look. For a clearly resolved droplet detection data for very high-throughput scenarios, the droplet spacing should be at least one droplet length or higher. Here, with a data sampling rate of 10 μs and well-spaced droplets, the theoretical droplet detection limit of the developed microwave system is 50 kHz.

Over a period of ten minutes, two million droplets were counted without missing any droplet. In order to assess the minimum sensible dielectric variation for detectable droplets, it is important to evaluate the resolution of the circuitry. An RMS noise level of 0.78 mV has been calculated over an interrogation time of 20 s. With this noise level, a resolution threshold of 0.026 dB in reflection coefficient was obtained. Since a resonant microwave sensor is designed and used in our study, we accumulate electromagnetic energy into small region, which is extremely sensitive to small changes. Likewise, utilizing the characteristic feature of microwaves, i.e., operation at GHz frequencies, allows working at shorter time scales. This gives a great opportunity and advantages over other detection techniques such as capacitive and electrochemical which operate at lower frequencies.

Droplet Content Sensing

Microwave sensing of droplet content was also carried out with the spiral resonator design. The spiral resonator was placed 8 mm away from the generator intersection. The microfluidic channel network and droplet generators are shown in Fig. 5 (a). Fluid pumping and droplet generation were controlled using a microfluidic pressure controller system (Fluigent MFCS-8C) which can provide more stable droplet generation²⁹. For this set of experiments, a double T-junction generator was used to alternatively generate droplet pairs with different materials encapsulated³³ such as type A and type B. The alternating generation works as follows. When one droplet (i.e. with content type A) is being generated in one of the T-junctions, it obstructs the main channel as it is growing and thus restricts the flow of the continuous phase, which causes a dramatic increase in the pressure upstream of the T-junction intersection. When the pressure increases to a critical value, it drives the continuous phase to neck and then pinch off the droplet³⁴⁻³⁶. After pinch off the remaining interface recoils back to the T-junction inlet. While this process is taking place, the other T-junction generator repeats similar droplet (type B) formation process. By well-tuned applied pressures, two alternating droplets can be formed sequentially (please see video S1 in the supplemental material). During the formation of droplets, although two pairs come to close proximity, they do not coalesce or cross-contaminate at certain operating regimes³³. This configuration has advantages over a simple Y-channel design in terms of operation of the two droplet generators and robustness. In addition, with this configuration there is no need to add a dilution stream in order to increase droplet spacing.

To demonstrate the sensitivity of the sensor and its potential to be applied in the area of biosensing with appealing features of no chemical and physical intrusion to the sample, some materials were strategically chosen. In particular, aqueous based solutions with slight differences in their concentration such as the potassium chloride solutions and glucose solutions used here, which result in similar dielectric constant and/or electric conductivity values, were chosen to demonstrate the sensitivity of the sensor. Two biochemical materials, fetal bovine serum that is a widely used serum-supplement for in vitro cell culture of eukaryotic cells and penicillin-streptomycin-neomycin antibiotic mixture (contain 5,000 units penicillin, 5 mg streptomycin and 10 mg neomycin/mL), that is widely used to prevent bacterial contamination of cell cultures due to their effective combined action against gram-positive and gram-negative bacteria, were chosen to demonstrate its potential for biosensing. Thawing fetal bovine serum and penicillin solution started in the fridge at 8 $^{\circ}\text{C}$, then completed

at room temperature while the bottles were swirled gently to mix the solution during the thawing process. D-(+)-Glucose and potassium chloride solutions were prepared in ultra-distilled water, and 2% fat content of milk was used. The reflection coefficient versus frequency characterization can be found in the supplemental material (Fig. S4).

In order to ensure that the microwave system can

differentiate droplets with small difference in dielectric properties, the experiments were carefully designed to eliminate the droplet size effect. As can be seen in Eq. (1), the frequency shift is a function of permittivity difference and the relative size of the droplet over the resonator. Considering that the electromagnetic field is accumulated in the sensing region, and the droplet width and height is confined with the channel,

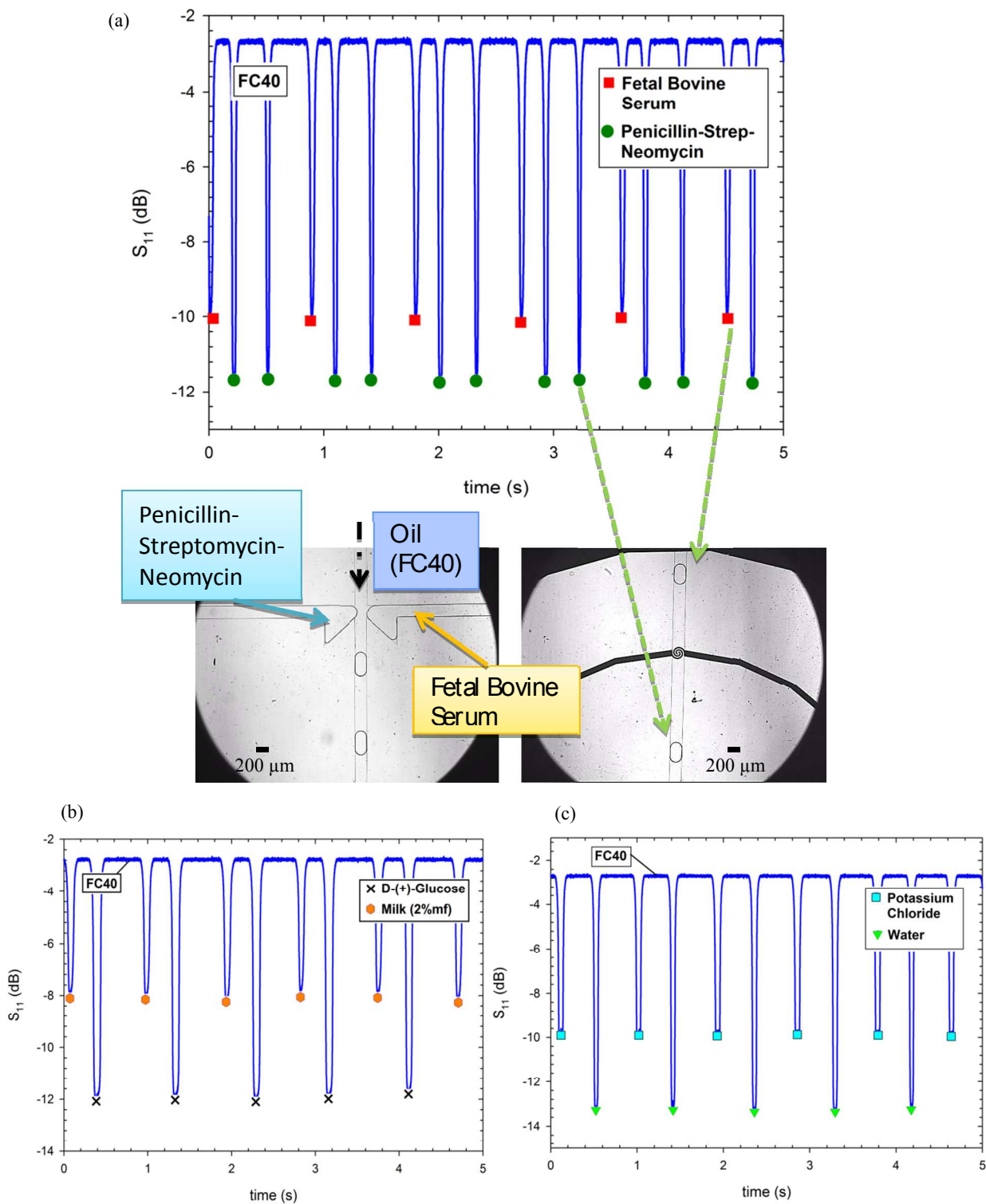


Figure 5. Label-free content sensing of individual droplets. (a) FBS-penicillin, (b) glucose (0.2g/ml)-milk, (c) water-potassium chloride (0.03g/ml) droplets.

droplet size has no effect on the reflection coefficient as long as its length is longer than the sensor region. This consideration ensures that the response of the sensor to different droplets is caused by dielectric property variation, namely by the specific droplet content.

In order to verify the sensing performance of the microwave system, ultra-pure water droplets were generated from both T-junction generators with FC40 oil as the continuous phase. The same sized droplets and different sized droplets were sensed with the same signal magnitude and the longer droplets resulted in wider signals due to their longer residence time in the sensing region (Figs. S5 and S6 in the Supplemental material). Subsequently, a set of droplet pairs of the same size were sensed which include a pair of Fetal bovine serum and penicillin-strep.-neomycin, a pair of D-(+)-glucose(0.2g/ml) and milk(2%mf), and a pair of potassium chloride(0.03 g/ml) and water droplets. Fig. 5 (a) shows the coordinated optical imaging and microwave sensing results while Fig. 5 (b) and (c) shows the microwave sensing results. More sensing results of droplet pairs with a combination of size and content differences

(AcPHF6) which is normally considered as a model for tau-protein aggregation in many assays was used as the peptide and Orange G which is one of the common inhibitors used in the traditional assay^{37,38} was chosen for this preliminary testing.

Figure 6 shows that the microwave sensor is able to differentiate the droplets with and without the mixture of peptide and inhibitor and the droplets with different concentrations of the inhibitor (Orange G), which are 0.665 mM and 0.332 mM respectively (Inhibitor_I and II respectively in the figure). The peptide concentration was kept at 0.316 mM and all droplets contain Thioflavin S (0.05mg/ml), which is a fluorescent indicator dye normally used in tau-aggregation assays. The samples were prepared in 4-morpholinepropanesulfonic acid (MOPS) buffer of 20mM with a pH of 7.2. There is only one set of droplets containing no mixture of orange G and AcPHF6, which is used as a base similar to the negative control in the traditional assay³⁷.

Please note that the sensing shown in Figure 6 only demonstrates that the developed microwave and microfluidic

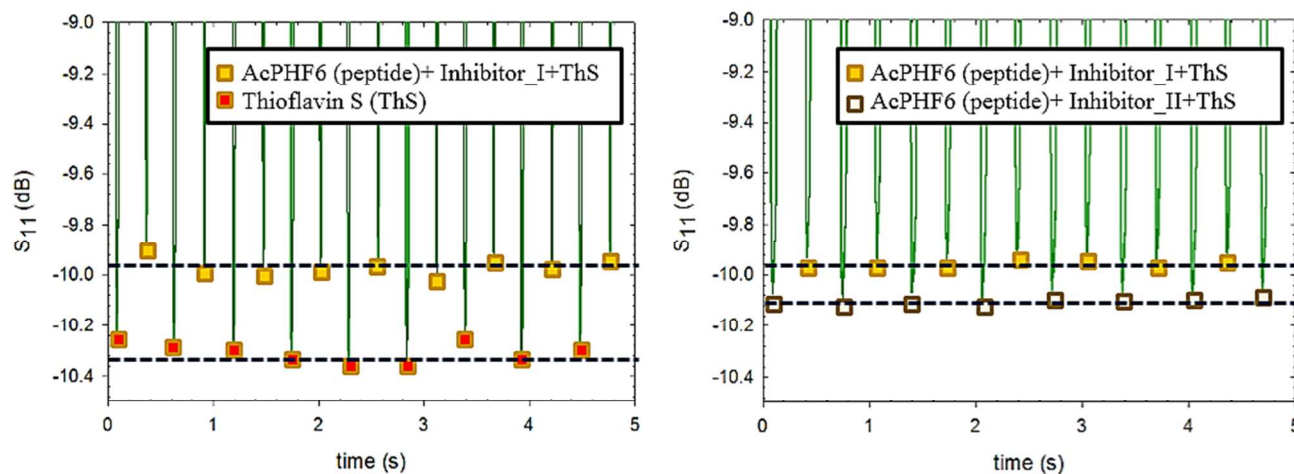


Figure 6. Demonstration of sensing of droplets involving AcPHF6 and Orange G which are the model peptide and inhibitor respectively used in traditional tau-aggregation assays that is linked to neurodegenerative disorders such as the Alzheimer's disease.

can be found in Figs. S5 and S6 in the Supplemental material.

The reflection coefficient difference between the fetal bovine serum droplets and penicillin droplets is -1.61 dB, which is 1.16 times lower, while -9.01 dB difference with the baseline of carrier oil FC40. As well, the difference between glucose and milk droplets is -4.02 dB, and between KCl and water droplets -3.45 dB. It is worthwhile that very low (-5 dBm) output excitation power was used in order to avoid any heating effect on droplets. These results show that our microwave module is very sensitive to nanoliter droplet permittivity contrast and can easily distinguish various droplet contents. We accomplished very high reproducibility. This microwave system can also be used with other bio-materials for content analysis or for synthesis and reaction monitoring. It should be noted that the demonstrated throughput of sensing is not high; however, it is limited by the throughput of droplet generation for the particular scenarios considered here rather the sensor which has been demonstrated for high throughput sensing as shown in Figure 4.

To demonstrate that this platform has the potential to be used as a tool for bioapplications, we applied it to perform a similar assay developed to screen inhibitors for tau-aggregation that is linked with neurodegenerative disorders such as the Alzheimer's disease (AD)^{37, 38}. The tau-derived hexapeptide

platform has the potential to serve as a tool for bioapplications. It is not a quantitative measure of the effects of the inhibitor on tau-aggregation because it is difficult to judge whether the signal difference is caused by the concentration of the inhibitor or the degree of peptide aggregation induced by the different inhibitor concentrations. To perform such an assay to quantitatively compare with the traditional assay would require systematic design of the microfluidic chip and microwave sensor and require further improvements on our sensor fabrication protocol as well to improve its sensitivity, which is beyond the scope of this study.

Conclusions

In this work, we demonstrated a system which consists of a custom microwave circuitry and microwave sensor integrated with microfluidic channel networks for label-free detection and content sensing of individual droplets. High-throughput and label-free droplet detection at kHz range has been realized as an alternative to optical methods while many other non-optical techniques mostly fail at kHz rates. As well, without any chemical or physical intrusion individual droplet contents have been distinguished successfully in real-time operation. This

system has significant advantages over optical detection systems for droplet microfluidics in terms of its infrastructure and operation cost, ease of use and portability for Lab-on-a-Chip applications. It also presents significant improvements compared to most electrical-based droplet detection systems in terms of its sensitivity and throughput. Therefore, it potentially facilitates the application of droplet microfluidics in point-of-care settings.

Acknowledgements

The authors gratefully acknowledge the support from Canada Natural Science and Engineering Council of Canada, Canada Foundation for Innovation, Canada Research Chair program, and Advanced Electrophoresis Solutions Ltd, through grants to Dr. Carolyn L. Ren. The authors also want to thank Prof. Eugenia Kumacheva at the University of Toronto and her PhD student, Mokit Chau for supplying surfactant and useful discussions. The authors would also like to thank Prof. Praveen P.N. Rao, Tarek Mohamed, Matthew Courtney, Xiaoming Chen and Sarah Chan for helpful discussion about drug screening testing for the Alzheimer's disease.

Notes and references

^a Department of Mechanical and Mechatronics Engineering, University of Waterloo, 200 University Avenue West, Waterloo, Ontario, N2L 3G1, Canada.

E-mail: c3ren@uwaterloo.ca; Fax: +1 519 885 5862; Tel: +1 519 888 4567 x 33030.

^b Department of Computer Engineering, Antalya International University, Universite Caddesi No:2, 07190 Antalya, Turkey.

† Electronic Supplementary Information (ESI) available. See DOI: 10.1039/b000000x/

- [1] L. Li, Q. Wang, J. Feng, L. Tong, and B. Tang, "Highly Sensitive and Homogeneous Detection of Membrane Protein on a Single Living Cell by Aptamer and Nicking Enzyme Assisted Signal Amplification Based on Microfluidic Droplets," *Anal. Chem.*, vol. 86, pp. 5101–5107, 2014.
- [2] E. W. M. Kemna, L. I. Segerink, F. Wolbers, I. Vermes, and A. van den Berg, "Label-free, high-throughput, electrical detection of cells in droplets," *Analyst*, vol. 138, no. 16, pp. 4585–92, 2013.
- [3] X. Ding, Z. Peng, S.-C. S. Lin, M. Geri, S. Li, P. Li, Y. Chen, M. Dao, S. Suresh, and T. J. Huang, "Cell separation using tilted-angle standing surface acoustic waves," *Proc. Natl. Acad. Sci. U. S. A.*, vol. 111, no. 36, pp. 12992–7, 2014.
- [4] Y. Chen, P. Li, P.-H. Huang, Y. Xie, J. D. Mai, L. Wang, N.-T. Nguyen, and T. J. Huang, "Rare cell isolation and analysis in microfluidics," *Lab Chip*, vol. 14, no. 4, pp. 626–45, 2014.
- [5] H. Zhu, G. Wang, D. Xie, B. Cai, Y. Liu, and X. Zhao, "Au nanoparticles enhanced fluorescence detection of DNA hybridization in picoliter microfluidic droplets," *Biomed. Microdevices*, vol. 16, no. 3, pp. 479–85, 2014.
- [6] M. T. Guo, A. Rotem, J. A. Heyman, and D. A. Weitz, "Droplet microfluidics for high-throughput biological assays," *Lab Chip*, vol. 12, no. 12, pp. 2146–55, 2012.
- [7] N. Wu, F. Courtois, R. Surjadi, J. Oakeshott, T. S. Peat, C. J. Easton, C. Abell, and Y. Zhu, "Enzyme synthesis and activity assay in microfluidic droplets on a chip," *Eng. Life Sci.*, vol. 11, no. 2, pp. 157–164, 2011.
- [8] L. Mazutis, J.-C. Baret, P. Treacy, Y. Skhiri, A. F. Araghi, M. Ryckelynck, V. Taly, and A. D. Griffiths, "Multi-step microfluidic droplet processing: kinetic analysis of an in vitro translated enzyme," *Lab Chip*, vol. 9, no. 20, pp. 2902–8, 2009.
- [9] H. Zhou, G. Li, and S. Yao, "A droplet-based pH regulator in microfluidics," *Lab Chip*, vol. 14, no. 11, pp. 1917–22, 2014.
- [10] E. Brouzes, M. Medkova, N. Savenelli, D. Marran, M. Twardowski, J. B. Hutchison, J. M. Rothberg, D. R. Link, N. Perrimon, and M. L. Samuels, "Droplet microfluidic technology for single-cell high-throughput screening," *PNAS*, vol. 106, no. 34, pp. 14195–14200, 2009.
- [11] R. Sista, Z. Hua, P. Thwar, A. Sudarsan, V. Srinivasan, A. Eckhardt, M. Pollack, and V. Pamula, "Development of a digital microfluidic platform for point of care testing," *Lab Chip*, vol. 8, no. 12, pp. 2091–104, 2008.
- [12] A. M. Foudeh, T. Fatanat Didar, T. Veres, and M. Tabrizian, "Microfluidic designs and techniques using lab-on-a-chip devices for pathogen detection for point-of-care diagnostics," *Lab Chip*, vol. 12, no. 18, pp. 3249–66, 2012.
- [13] M. Robert de Saint Vincent, S. Cassagnère, J. Plantard, and J.-P. Delville, "Real-time droplet caliper for digital microfluidics," *Microfluid. Nanofluidics*, vol. 13, no. 2, pp. 261–271, 2012.
- [14] J. Lim, P. Gruner, M. Konrad, and J.-C. Baret, "Micro-optical lens array for fluorescence detection in droplet-based microfluidics," *Lab Chip*, vol. 13, no. 8, pp. 1472–5, 2013.
- [15] L. Mazutis, J.-C. Baret, and A. D. Griffiths, "A fast and efficient microfluidic system for highly selective one-to-one droplet fusion," *Lab Chip*, vol. 9, no. 18, pp. 2665–72, 2009.
- [16] M. Fukuyama, Y. Yoshida, J. C. T. Eijkel, A. van den Berg, and A. Hibara, "Time-resolved electrochemical measurement device for microscopic liquid interfaces during droplet formation," *Microfluid. Nanofluidics*, vol. 14, no. 6, pp. 943–950, 2012.
- [17] G. D. M. Jeffries, R. M. Lorenz, and D. T. Chiu, "Ultrasensitive and High-Throughput Fluorescence Analysis of Droplet Contents with Orthogonal Line Confocal Excitation," *Anal. Chem.*, vol. 82, no. 23, pp. 9948–9954, 2010.
- [18] N. M. M. Pires, T. Dong, U. Hanke, and N. Hoivik, "Recent developments in optical detection technologies in lab-on-a-chip devices for biosensing applications," *Sensors (Basel)*, vol. 14, no. 8, pp. 15458–79, 2014.
- [19] J. Wu and M. Gu, "Microfluidic sensing: state of the art fabrication and detection techniques," *J. Biomed. Opt.*, vol. 16, no. 8, p. 080901, 2011.
- [20] J. Sochor, J. Dobes, O. Krystofova, B. Ruttkay-nedecky, and P. Babula, "Electrochemistry as a Tool for Studying Antioxidant Properties," *Int. J. Electrochem. Sci.*, vol. 8, pp. 8464–8489, 2013.
- [21] K. Mitton and J. Trevithick, "High-performance liquid chromatography-electrochemical detection of antioxidants in vertebrate lens: glutathione, tocopherol, and ascorbate," *Methods Enzym.*, vol. 233, pp. 523–539, 1994.
- [22] N. Wongkaew, P. He, V. Kurth, W. Surareungchai, and A. J. Baumner, "Multi-channel PMMA microfluidic biosensor with

- integrated IDUAs for electrochemical detection,” *Anal. Bioanal. Chem.*, vol. 405, no. 18, pp. 5965–74, 2013.
- [23] C. Elbuken, T. Glawdel, D. Chan and C.L. Ren, "Detection of Microdroplet Size and Speed Using Capacitive Sensors", *Sens Actuator A: Phys*, 171, pp. 55-62, 2011.
- [24] E.V. Moiseeva, A.A. Fletcher and C.K. Harnetten, "Thin-film electrode based droplet detection for microfluidic systems" *Sensors and Actuators B: Chemical*, 155, pp. 408-414, 2012.
- [25] M. S. Boybay, A. Jiao, T. Glawdel, and C. L. Ren, "Microwave sensing and heating of individual droplets in microfluidic devices.," *Lab Chip*, vol. 13, no. 19, pp. 3840–6, 2013.
- [26] D. M. Pozar, *Microwave Engineering*, 4th Ed. John Wiley & Sons, Ltd, 2012.
- [27] N. Suwan, "Investigation of RF Direct Detection Architecture Circuits for Metamaterial Sensor Applications," University of Waterloo, 2011.
- [28] G. F. Engen, "The Six-Port Reflectometer: An Alternative Network Analyzer," *Microw. Theory Tech.*, IEEE Trans., vol. 25, no. 12, pp. 1075–1080, 1985.
- [29] F. M. Ghannouchi and A. Mohammadi, *The Six-Port Technique with Microwave and Wireless Applications*. Artech House Publishers, 2009.
- [30] J. Ardizzoni and D. Falls, "A Practical Guide to High-Speed Printed Circuit Board Layout," Analog Devices Inc., 2005.
- [31] T. Glawdel and C. L. Ren, "Global network design for robust operation of microfluidic droplet generators with pressure-driven flow," *Microfluid. Nanofluidics*, vol. 13, no. 3, pp. 469–480, 2012.
- [32] J. Kim, A. J. deMello, S.-I. Chang, J. Hong, and D. O'Hare, "Thermoset polyester droplet-based microfluidic devices for high frequency generation.," *Lab Chip*, vol. 11, no. 23, pp. 4108–12, 2011.
- [33] B. Zheng, J. D. Tice, and R. F. Ismagilov, "Formation of droplets of alternating composition in microfluidic channels and applications to indexing of concentrations in droplet-based assays," *Anal. Chem.*, vol. 76, no. 17, pp. 4977–82, 2004.
- [34] C. N. Baroud, F. Gallaire, and R. Danga, "Dynamics of microfluidic droplets.," *Lab Chip*, vol. 10, no. 16, pp. 2032–45, 2010.
- [35] T. Glawdel, C. Elbuken, and C. Ren, "Passive droplet trafficking at microfluidic junctions under geometric and flow asymmetries.," *Lab Chip*, vol. 11, no. 22, pp. 3774–84, 2011.
- [36] T. Glawdel, C. Elbuken, and C. L. Ren, "Droplet formation in microfluidic T-junction generators operating in the transitional regime. I. Experimental observations," *Phys. Rev. E*, vol. 85, no. 1, p. 016322, 2012.
- [37] T. Mohamad, T. Hoang, M. Jelokhani-Niaraki and P.P.N. Rao, "Tau-derived-hexapeptide VQIVYK aggregation inhibitors: nitro catechol moiety as a pharmacophore in drug design" *ACS Chemical Neuroscience*, (4) 12, pp. 1559-1570, 2013.
- [38] S. N. Haydar, H. Yun, R. G. W. Staal and W. D. Hirst, "Small-molecule protein-protein interaction inhibitors as therapeutic agents for neurodegenerative diseases: recent progress and future directions." *Annu. Rep. Med. Chem*, 44, pp. 51-69, 2009.